A UNITED STATES DEPARTMENT OF COMMERCE PUBLICATION

NOAA Technical Memorandum ERL WMPO-3

U.S. DEPARTMENT OF COMMERCE
NATIONAL OCEANIC AND ATMOSPHERIC ADMINISTRATION
Environmental Research Laboratories

A Preliminary View of Storm Surges Before and After Storm Modifications

C. P. JELESNIANSKI
A. D. TAYLOR

NHRL-102

U.S. DEPARTMENT OF COMMERCE
National Oceanic and Atmospheric Administration
Environmental Research Laboratories

NOAA Technical Memorandum ERL WMPO-3

A PRELIMINARY VIEW OF STORM SURGES BEFORE AND AFTER STORM MODIFICATIONS

C. P. Jelesnianski
Techniques Development Laboratory
National Weather Service
National Oceanic and Atmospheric Administration
Silver Spring, Maryland

A. D. Taylor
Air Resources Laboratory
Environmental Research Laboratories
National Oceanic and Atmospheric Administration
Silver Spring, Maryland

Weather Modification Program Office
Boulder, Colorado
May 1973

TABLE OF CONTENTS

	Page
ABSTRACT	1
1. INTRODUCTION	1
2. SOME PERTINENT DEFINITIONS	2
3. SURGES FROM ANALYTICALLY DEFINED DRIVING FORCES	3
4. SURGES COMPUTED WITH IN-SITU WIND OBSERVATIONS	8
5. SUMMARY AND CONCLUSIONS	14
REFERENCES	16
APPENDIX A - MAXIMUM SURFACE WIND	17
APPENDIX B - CRITICAL STORM SIZES AND VECTOR STORM MOTIONS	20
APPENDIX C - COMPUTING PRESSURE AND INFLOW ANGLE PROFILES FROM A GIVEN WIND PROFILE	23

A PRELIMINARY VIEW OF STORM SURGES BEFORE AND AFTER STORM MODIFICATIONS

C. P. Jelesnianski
and
A. D. Taylor

Storm surges are computed numerically with a two-dimensional dynamic surge model, before and after storm modifications. The driving forces used to generate the surges are derived from wind profiles, used here in two different forms. First, a continuous analytic form is used. Second, tabulated wind values from Doppler wind observations measured at 12,000 ft altitude are used; these winds are incremented at 1 n mile intervals from the storm's center.

The resulting computations imply that the peak surge on the open coast is not always monotonically related to the parameter, maximum wind speed of the storm. In fact, with the analytic wind profile, the peak surge may increase or decrease according to the manner in which the other storm parameters are affected by the change in maximum wind speed. From the tabulated wind profiles, it is found that the shape of the wind profile has an effect on the peak surge and is separate from the effects of maximum wind, pressure drop, and size scale.

1. INTRODUCTION

It may be possible to internally modify tropical storms through external activity, such as cloud seeding (Simpson et al., 1963; Gentry, 1970; Rosenthal, 1971). Storms are also naturally modified when moving within surrounding meteorological systems, across sea-surface temperature gradients, etc. For such cases, the newly modified storm may give a significantly different storm surge. We are interested in this problem because the storm surge can--and at times does--account for a significant fraction of the total storm damage.

The storm's driving forces form a circulating mound of water that can precede, lag, or remain directly under the storm as it traverses the Continental Shelf. The position of this mound, relative to the storm's center, depends on the storm's motion and size, as well as the geometry of the ocean bottom. Eventually, the mound impinges on the shoreline to form abnormal tides or surges on the open coast. To investigate this phenomena as it relates to storm modification, we make

use of a dynamic storm model (Jelesnianski, 1967). This model was redesigned to accept general forces, and in particular, observed driving forces given in tabulated form.

Our primary goal here is not to give a definitive yes/no answer to the practical question, "Do surges increase/decrease with storm modification?" The issue is too complicated for simple answers. To tackle the question in a preliminary manner, we isolate our system and consider surge changes due solely to storm modification. To do this, we fix--throughout this paper--the bathymetry of the Continental Shelf, the vector storm motion, and latitude of landfall. In this way, we avoid complications and external effects due to varying shelf bathymetry, changes in landfall, varying storm motion, etc. We point out, however, these complications and external effects can have greater significance for surge changes than meteorological modifications. Our results in this study are very specialized and only touch on the total problem.

Two types of meteorological input data are used to compute storm surges on the open coast. The first uses an analytic wind profile (Jelesnianski, 1966) to form driving forces, and we call this a model wind profile. We modify the profile in some analytic fashion, compute the surges with our dynamic surge model - both before and after storm modification - and then compare the resulting surges on the open coast. There are objections here inasmuch as the model profile, and modifications, may not sufficiently represent natural conditions. We offer the results from this approach as a guide for the contemplation of surge changes. The principal lesson derived is that changes in only one parameter, such as the maximum wind, are insufficient to determine whether the storm surge will increase or decrease. A decrease in maximum wind may be associated with either a decrease in surge or an increase, or neither, depending on how the other storm parameters are changed.

Second, we use in-situ observations of wind to form driving forces, both before and after storm modification, and compute coastal storm surges. This is still an idealized situation, however, because the very few available observations were made at 12,000 ft altitude. At this time, we do not know how to represent surface forces solely from high-altitude wind observations. We bypass this impasse simply by translating the observed winds to the surface. We offer the results of this approach as a guide for contemplating surge changes. Our principal finding here is that the shape of the wind profile has much to say about the magnitude of the peak surge, even apart from the maximum wind parameter.

2. SOME PERTINENT DEFINITIONS

There are two driving forces that generate surges on the sea surface: surface wind stress and pressure gradient force; these act parallel and normal to the sea surface, respectively. Their relative importance depends on the water depth and changes from point to point. We formulate

the driving forces from analytic/observed wind-speed profiles, appendix C. Each driving force, acting alone on the sea, generates its own surges. Our dynamic surge model is a linear one; hence, the surges due to wind and pressure can be superimposed without interaction.

The assemblage of surges on the coast, for any given time, is called a coastal storm surge profile. The assemblage of highest water at each point on the coast, for all time, is called a coastal storm surge envelope. The highest surge on the envelope is called the peak surge.

In our dynamic surge model the local surface wind-stress driving force varies with the local wind speed squared. One might then expect the peak surge on the profile to be directly and monotonically related to the maximum wind. Is this true? Yes and no, depending on circumstances. In part, the circumstances are size of storms, the distribution of the wind about the storm, pressure drop of storm, basin bathymetry, and vector storm motion. To simplify our presentation, we will constrain all our storms to traverse a standard basin with a standard vector storm motion. These are defined as:

Standard basin: A basin with a straightline coast, whose depth profile seaward is one-dimensional, and whose bathymetry is a linear slope (Jelesnianski, 1972). This can be viewed as a hypothetical mean basin for all of the U. S. coasts.

Standard storm motion: A storm motion of 15 mph and a track normal to the coast from sea to land. The storm must landfall at some coastal point; we arbitrarily set this at latitude 30°N. This motion can be viewed as a hypothetical mean motion for all storms.

With these constraints, we concern ourselves with storm conditions and modifications, exclusively.

3. SURGES FROM ANALYTICALLY DEFINED DRIVING FORCES

To study storm surges, it is not enough to specify the maximum wind speed of a tropical storm. Additional meteorological parameters such as pressure drop and storm size are indeed helpful but still insufficient. We need to know the distribution of wind from the storm center, i.e., the wind profile.

In our tropical storm model (Jelesnianski, 1966), we make a bold but most convenient assumption: the sea surface wind profiles for stationary tropical storms are similar. This is illustrated in figure 1 where we have nondimensionalized our wind[1] speed W, and the distance 'r' from

[1]Our wind speed W, and the maximum wind, W_M, at distance R from the storm center are a special kind of average wind. For a discussion of winds, see appendix A.

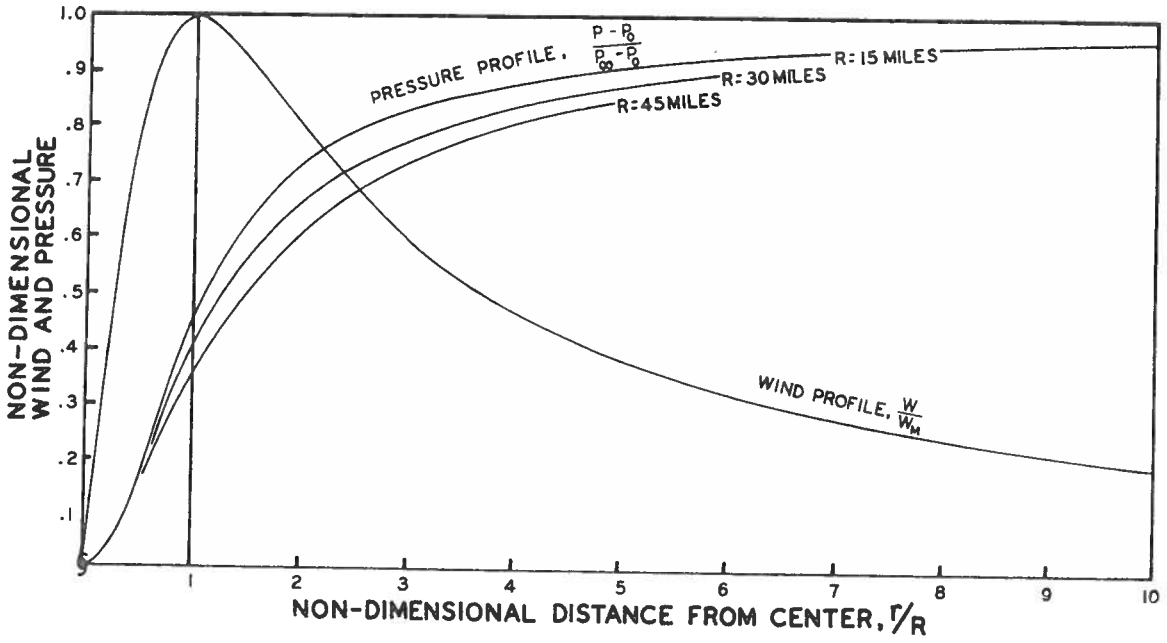

Figure 1. Nondimensional wind and pressure profiles from center of a stationary model storm. The wind profile is similar for all storms. The pressure profile is similar only if R, the radius of maximum wind, is constant. 'r' is radial distance from the storm center.

storm center; we call this our model wind profile. Certainly, normalized wind profiles for natural storms do not always parallel figure 1; this is readily obvious for a point vortex storm or the opposite extreme $R \to \infty$, but for the limited range used in this report, $10<R<50$ miles, this may be an adequate approximation. It would be nice if the pressure profiles were also similar for all storms, but this is not to be, because of the changing curvature of the pressure isobars at distance R from the storm center, i.e., the larger R the less curvature. For constant R, the nondimensionalized pressure profiles in figure 1 are nearly similar for any $\Delta P = P_{00} - P_0$ (where P_{00} is ambient air pressure surrounding the storm and P_0 is the storm's central pressure); we say nearly similar because surface friction and Coriolis weakly enter the picture, and these do not have such similarities.

The ratio $\Delta P/R$ is a rough measure of the pressure gradient. For storm surge generation with our model storm, it is of some significance whether a change in pressure gradient is due to a change in ΔP with R

unchanged, or to a change in R with ΔP unchanged; this is so even if the same change in pressure gradient is produced. The reason for this distinction is that, at constant R, the scale size of the storm is unchanged while the intensity is altered.

Now, if the driving forces are similar for sets of storms, that is constant R, then the sets of generated surge profiles[2] are also similar; this assumes basin and vector storm motion to be the same.

Consider the special case where R is held constant, but maximum wind is reduced; ΔP must then become smaller, see figure 1 and appendix A. For this case, the three normalized profiles, wind, pressure, and surge, remain similar; i.e., no changes occur in horizontal scale size. Hence, a reduction in maximum wind means a reduction of values throughout the three profiles, and in particular a reduction of the peak surge.

Consider now the special case where ΔP is held constant but maximum wind is reduced; the scale size R must then become larger, see figure 1. Contrary to the previous case, the pressure profiles are no longer similar when R is altered (fig. 1), and for the pressure gradient force our similarity argument breaks down. We can no longer argue for a reduction of peak surge with a reduction of maximum wind.

Now in most cases with tropical storms, the generated surge due to wind stress is much greater than from pressure gradient force. Hence, with similar wind profiles, we are inclined to assume that surge profiles will remain similar; i.e., the surge decreases/increases directly with maximum wind. Things are not this simple, however; what we need to keep in mind is that a scale change in storm size requires a compensating change in basin size[3] and storm motion to maintain similarity of surge profiles. But, because our basin and storm motion have been fixed, we expect changes in the surge profile with changes in storm size. How does the surge react? To answer this question, we use the dynamic surge model and storm model to compute figure 2.

Figure 2--which assumes a model wind profile--is a nomogram that relates R, ΔP, W_M, and SS; size of storm, pressure drop, maximum wind, and peak storm surge. We need only to specify any two of these parameters, such as R and ΔP to use it, but note that the peak surge SS is valid only in a standard basin for a standard storm motion. An

[2]We have not portrayed any surge profile in figure 1. The omission is purposeful. The profile is a function of time, and as such it builds and abates with time as the storm traverses the Continental Shelf.

[3]By basin size we mean a length, derived by dividing a typical depth in the ocean by the slope of the Continental Shelf; hence, to change the size we would need to consider a change in the slope of the Continental Shelf.

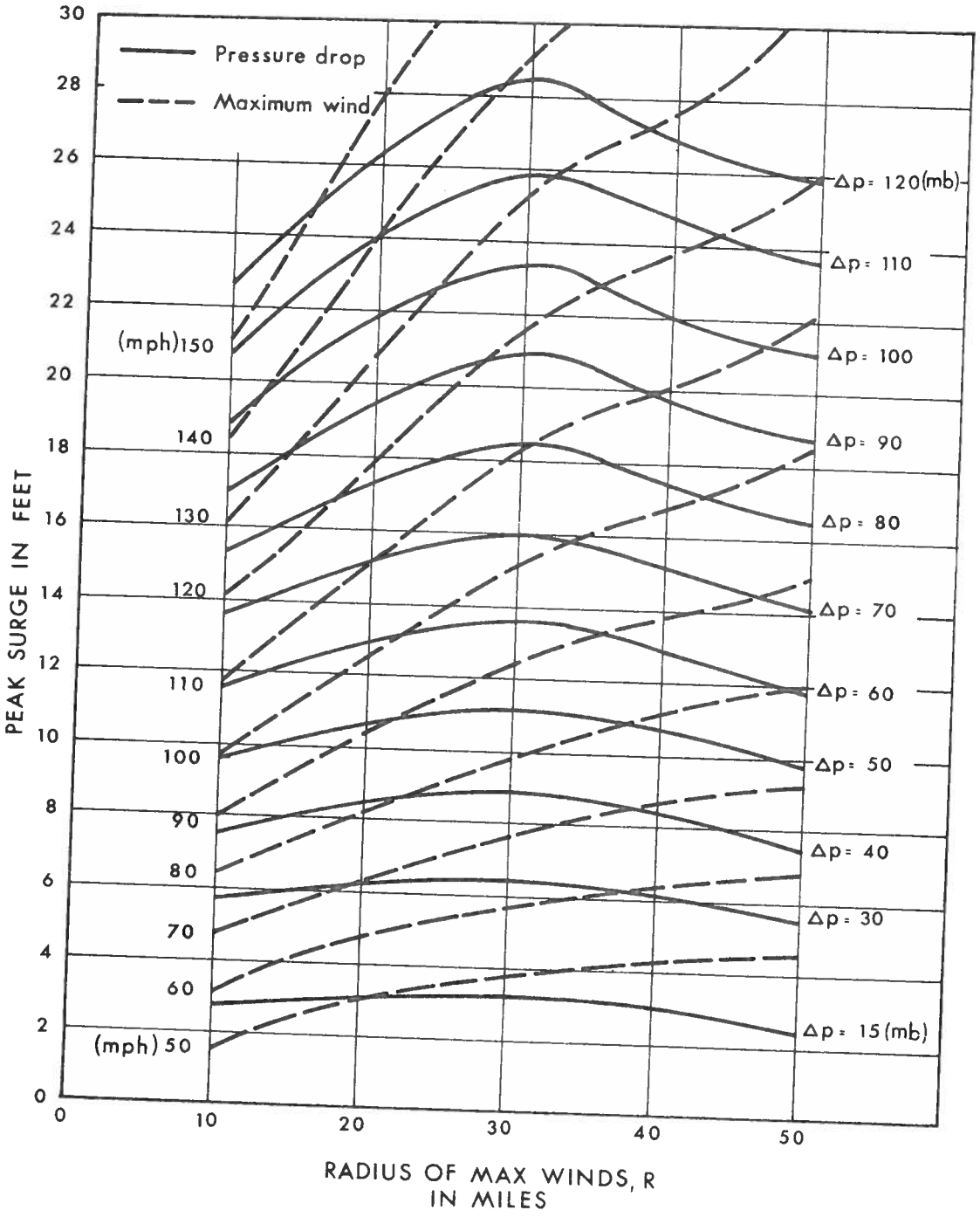

Figure 2. A nomogram of peak surge on the open coast as a function of pressure drop and radius of maximum wind. A standard basin (72 miles wide), standard vector storm motion, and model wind profile were used to form the nomogram. For reference, the maximum wind of the model storm (see fig. A1) is also displayed.

examination of figure 2 shows that it is impossible to change W_M without changing ΔP or R, or both; however, a specified change in W_M does not in itself tell which one is changed or by how much. This is of crucial importance as we show with an example. Suppose we have an initial state of ΔP = 80 mb and R = 18 miles. The nomogram gives immediately W_M = 120 mph and SS = 16.8 ft. Now suppose the wind speed is decreased by 10 mph; what is the final state? We can reach a final state by many paths, but consider only two of them; let either ΔP or R stay constant as the winds decrease. These states are:

	Initial	ΔP cnst Final	R cnst Final
ΔP	80	80	68
R	18	31	18
W_M	120	110	110
SS	16.8	18.3	14.3

Note the increase in surge with decrease in maximum wind in the middle column.

Suppose now the initial state is the middle column above and the wind is again decreased by 10 mph to a final state. Then,

	Initial	ΔP cnst Final	R cnst Final
ΔP	80	80	67
R	31	43	31
W_M	110	100	100
SS	18.3	17.1	15.5

So, if you want to decrease the peak surge by decreasing the maximum wind, it is better if R--rather than ΔP--remains constant. Merely decreasing the maximum wind is not sufficient in itself to decrease the peak surge. It is even possible, under some circumstances, to decrease the peak surge by increasing the maximum wind.

For moving storms, and with ΔP constant, the peak surge can vary either way when R is modified. Here an increase in R generates larger surges until a critical R is reached; thereafter the peak surge decreases. The argument is reversed by decreasing R (appendix B). We mention a significant by-product; with increasing R the coast length affected by significant surges is also increased, and especially so if the peak surge also increases. Similarly, the potential for inland inundation is greater with increasing storm size.

Of course, the above dynamics do not occur in nature with such simplicity. These are only convenient modeling techniques that appear to explain observed surges reasonably well. Other storm models may explain the observed surges as well or better. In particular, the assumption of a similar wind profile for all tropical storms is questionable.

Remember that storms do not jump at once from initial to final state; it takes time to do this. Conceivably, the storm surge could be vitiated if landfall occurs during the transient period between storm states, i.e., while the driving forces on the sea--following the storm--are undergoing accelerative changes.

In addition to wind and pressure profiles, there is also the inflow angle profile, i.e., the inflow angle of wind on concentric circles about the storm center. This information is necessary to determine direction of surface stress. We have not shown any profiles for this angle because they have no simple similarities such as the wind and pressure profiles. Large changes in the inflow angles give small changes in the computed surge, all other things being the same. The inflow angle is strongly dependent on friction coefficients, whose numerical values vary slowly with storm parameters. It is possible that for huge changes in meteorological parameters, the total surge change that results when using figure 2 is improper because of poorly designed friction coefficients; however, for the small changes in storm parameters with which we are dealing, the surge change due solely to changing inflow angles is at most minor. That is, large or global changes in figure 2 might be suspect, but small or local changes are qualitatively correct.

4. SURGES COMPUTED WITH IN-SITU WIND OBSERVATIONS

Some of the most detailed wind observations were made inside Hurricane Debbie, August 1969. We were supplied with wind speed profiles, tabulated at 1 n mile intervals, figure 3 (we have interpolated at 1 statute mile intervals for convenience), before and after seeding operations by Project STORMFURY.

Wind speed profiles in the figure are Doppler wind observations--measured along rays from the storm center outward--from aircraft at 12,000 ft. The observations were in the most vigorous storm quadrant;

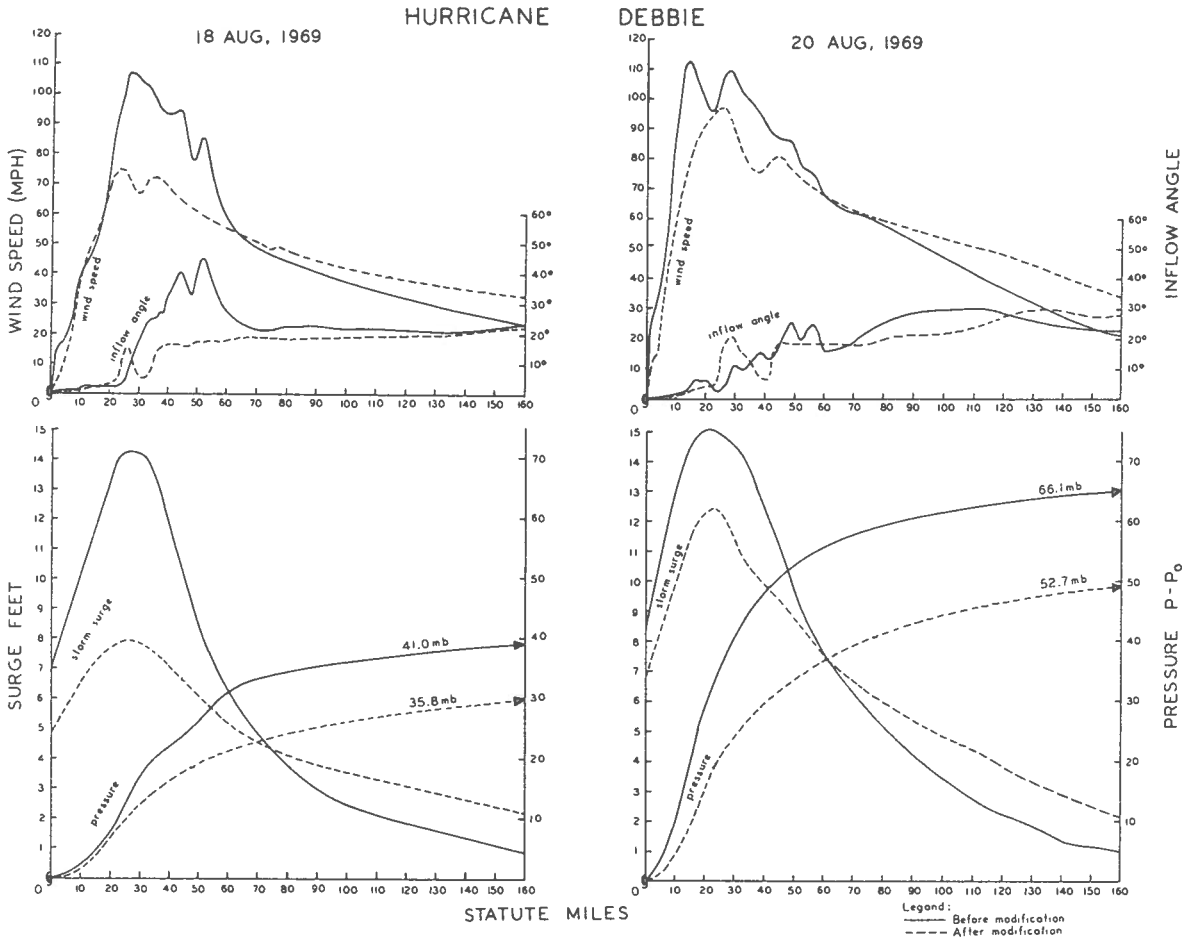

Figure 3. Profiles of observed wind speed and computed inflow angle, pressure, and open coast surge for Hurricane Debbie (1969) before and after storm modifications. The surge is the envelope of high water on the coast for all times. The numbers on the pressure profiles are pressure drop in millibars.

i.e., in the region of maximum winds for a moving storm; they do not represent a stationary storm. The one-quadrant observations were heavily accented along the core of the storm; i.e., about 60 miles from the storm center. We make no comments on the dynamics of the storm modifications, the noise levels, the smoothing techniques used to derive the profile, etc.; we merely accept the winds as given.

The given observations extend 230 statute miles from the storm center; we extend them farther by allowing the wind to decay exponentially. We also pretend the winds on the sea surface are the same as

these (12,000 ft), and that they are for a stationary storm. Now, before driving forces can be input into the dynamic surge model, we need somehow to derive the inflow angle of the wind on concentric circles about the storm center, the pressure profile, and hence the pressure gradient. A method for doing this (using tabulated wind data) is given in appendix C; the results are shown in figure 3. Note the gyrations along the profiles of inflow angle that correspond to secondary maxima on the wind profiles; we assume that a given wind profile results from a balance of forces, and the inflow angle is calculated from that balance. Hence, a complicated wind profile means a complicated inflow angle profile.

The surges computed by the dynamic surge model, using the given observed winds to determine driving forces, are also shown in figure 3. We display there the envelope of high-waters on the coast; i.e., the envelope of all surge profiles against time. The peak surge, computed before and after storm modification, decreased by 45 percent on the 18th of August and 17 percent on the 20th of August; the computed pressure drop decreased by 13 percent and 20 percent, respectively. From the chaotic appearance of the wind profiles, it is difficult to directly ascertain changes in storm sizes.

Referring to figure 2, we can easily decrease the surge by 17 percent with our similarity wind profile, the pressure drops for Debbie on the 20th of August, and changing storm size. Now, in no case can we decrease the surge by 45 percent with our similarity wind profile, the pressure drops for Debbie on the 18th of August, and changing storm size; this means that the large decrease in surge is due in part to wind profiles that are dissimilar when normalized.

If the shape or distribution of measured wind profiles differs substantially from our model wind profile, but all other things remain the same, then the computed surges from both profiles can also differ substantially. It is desirable, therefore, to have on hand some assessments on how surges will change if the shape of the wind profile changes. To investigate this situation, at least qualitatively, we form a standard for comparing measured wind profiles against the model wind profile. We do this by selecting the model wind profile that comes closest to the measured profile in a least-squares sense. That is, we choose the parameters of maximum wind speed and radius of maximum wind for our model wind profile so that--on the average--the squares of the differences between the model wind and measured wind[4] are minimized. This is comparable with selecting a square that 'best fits' a circle on the grounds of having equal area or equal perimeter, even though it may not appear to resemble the circle very well.

[4]We recall that the observations extend only to 200 n miles (230 st miles) from the storm center, and the best fit process was limited to this distance.

If the observed wind profile is a complicated shape and form, then the best fit model wind profile could be distinctively different (i.e., a poor representation). It does not follow that the pressure and inflow angle profiles--for the best fit wind profile--will also be the best fit; in fact, the pressure drop for the best fit storm may be substantially different from that of the observed storm.

Since model wind profiles are similar in shape, a change of scale in both distance and speed can cause them to lie on top of each other; the same changes in scale on measured wind profiles will then allow a comparison. The result is that we can graph the observed and best fit model storms--before and after seeding--as if they had the same size and intensity, then the remaining discrepancies highlight the different distribution of wind speeds.

If we normalize the observed wind profiles in accordance with the best fit model[5] profile, we get a comparison of the shape of the observed wind profiles before and after seeding. Figure 4 illustrates such fits, and we immediately see two types of conditions:

1. The observed profile is peaked relative to the best fit model profile.

2. The observed profile is flattened relative to the best fit model profile.

In addition to being peaked, the profiles are also skewed; i.e., in the absence of skew, a flattened profile should have shoulders on either side of the model profile, and otherwise for a peaked profile. Therefore, we see two more conditions:

1. The observed profile is skewed to the right of the best fit model profile.

2. The observed profile is skewed to the left of the best fit model profile.

Based on empirical computations, we can say tentatively that:

A. The computed peak surge from a peaked wind profile skewed to the right is larger than from the best fit model profile.

B. The computed peak surge from a flattened wind profile skewed to the left is smaller than from the best fit model profile.

[5]The shape of the model profile is only a guess, based on subjective experience. We await with pleasure a determination for an alternative shape of the wind profile, based on observations or scientific studies.

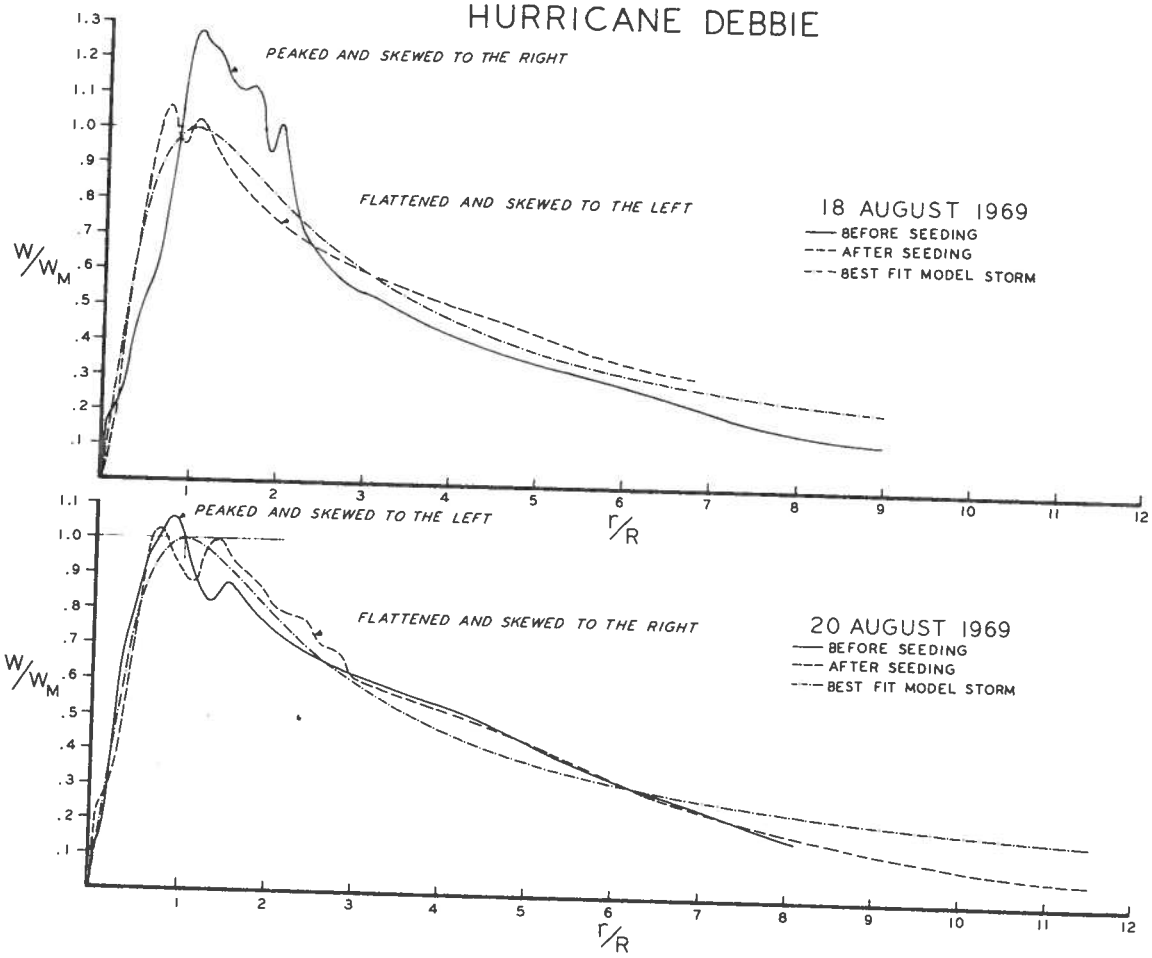

Figure 4. A comparison of observed and model wind profiles for Hurricane Debbie. The profiles are normalized with respect to the model wind profile. The model profile is a best fit in least-squares sense.

These qualitative statements are rough and of a subjective nature; we consider them useful only if the peaked, flattened, or skewed condition is substantial. In figure 4[6], the normalized observed wind profile--before seeding on the 18th of August--is highly peaked and highly skewed to the right, and its computed peak surge is substantially larger than

[6] In all the surge computations, both driving forces--pressure gradient force and wind stress--were used.

that resulting from the best fit model storm (see A above); the normalized observed wind profile--after seeding on the 18th of August--is slightly flattened and slightly skewed to the left, and its computed peak surge is only slightly smaller than that which results with the best fit model storm (see B above). The remaining two wind profiles--before and after seeding on the 20th of August--have some peaked and skewed conditions in the normalized observed wind profiles, but they do not act in concert for A and B above; the computed surges do not differ substantially from those computed with the best fit model storm; see table 1.

Table 1. Computed surges for Hurricane Debbie data and a best fit model storm.

		ΔP (mb)	R (st miles)	W_M (mph)	SS (ft)
	18 August 1969				
before modification	observed	41.0	27.0	107.5	14.3
	best fit	46.8	25.9	84.3	10.4
after modification	observed	35.8	?	?	7.9
	best fit	37.3	33.8	70.6	8.2
	20 August 1969				
before modification	observed	66.1	?	?	15.1
	best fit	69.2	20.0	109.5	14.9
after modification	observed	52.7	25.0	97.0	12.5
	best fit	56.2	28.6	91.9	12.6

In figure 4, note that the first observed wind profile (18 August, before seeding) is the only one that differs substantially from the best fit model profile; in table 1, note that only for this observed profile do the peak surge[7] and pressure drop substantially differ from the best fit model profile. This suggests that if observed wind profiles do not grossly differ from our best fit model wind profile, then the computed surges using either profile may be representative.

[7]The pressures and surges were computed, not observed.

We remind the reader that there are two driving forces that generate surges: the pressure gradient force and the wind stress. The wind stress accounts for most of the surge activity in the region of peak surge, and the surge is insensitive to mild changes in inflow angles. Hence, we require a good representation of the wind profile. On the other hand, a poor representation of the pressure and inflow angle profiles will, at most, only mildly affect the surges. For these reasons, we compared surges from the best fit model with observed wind profiles, regardless of the end disposition of the other profiles. We remark on the following:

1. In operational forecasting of surges, the wind profile is unknown, but we do know something about the pressure drop and storm size. If a model wind profile is described by these two parameters and it adequately represents the real wind profile, then it is possible to distribute the winds from the storm center outwards. Note: the model wind profile here is at the mercy of the measured parameters. If the real wind profile differs radically from the model wind profile, then our surge forecast can be seriously in error; see the wind profiles (pressure drops and storm sizes), figure 4 and table 1, for Hurricane Debbie on 18 August before seeding.

2. In assessing surge changes due to storm modifications, the wind profiles were known[8] but the pressure and inflow angles were not specified for these computations. A balance of forces--using the observed winds as input data--was then used to determine the unspecified profiles (appendix C). Thus, the unspecified profiles (including pressure drop) were at the mercy of the observed wind profile.

3. In best fit model wind versus observed wind profiles, the resulting pressures and inflow angles for each wind profile can differ (this can occur even with good representation between the two wind profiles). In itself this is not serious, for the wind stress accounts for the lion's share of surges in the region of peak surge. Note: the best fit model wind profile here is at the mercy of the observed wind profile.

5. SUMMARY AND CONCLUSIONS

One must stoutly resist the temptation to use the maximum wind speed of a tropical storm as the sole and direct measure of peak surge generated by the storm. When dealing with storm modifications, the resulting change in maximum wind speed alone is not a particularly good indicator for change in peak storm surge; it is even possible for the

[8]At least at aircraft altitude, for one storm quadrant or a limited portion of it.

sense of the change in peak surge to be contrary to the change of maximum wind. At least one additional parameter is imperative.

It may also prove unfruitful to consider changes in several meteorological parameters as indicators of storm surge activity. We point out that the form of the wind profile, i.e., the distribution of wind from the storm center, is highly important for surge generation; however, it is possible to have a rich variety of wind speed profiles with the same meteorological parameters. If it were possible to specify the form of the wind profile with only a few simple meteorological parameters, then it would be possible to specify surge changes due solely to modifications of these parameters. This was done in the main report as a special case when we assumed that all wind profiles are similar.

At present we cannot give hard and fast rules on surge modification due solely to storm modifications. This is so because the form of wind profiles is not universally known. Using particular observed wind profiles, such as for Hurricane Debbie (1969), to generate surges in our dynamic model is interesting and instructive, but inconclusive for general considerations; it does point out, however, the importance of the form or shape of wind profiles.

The tendency to concentrate on meteorology for indicators of storm surge activity, while ignoring oceanic shelf conditions, can be dangerous. If specific oceanic shelf conditions were to be considered, then a rich harvest of intriguing possibilities for storm surge amelioration is possible. In this study, constant-slope basins were used, but there are many areas along the U. S. Continental Shelves where the ocean depth topography changes dramatically in two dimensions. In these areas, peak surge on the coast will also vary dramatically.

If a storm increases in size so that location of peak surge changes, and if the shelf topography varies, then the newly positioned peak surge can change drastically in height. An example of such an area lies between Gulfport, Mississippi, and Pensacola, Florida. In this area, Hurricane Camille (1969), which was an ordinary sized storm for the Gulf of Mexico, gave a record surge in the Gulfport area; however, if the storm had been larger with maximum winds farther from its center, the peak surge would have occurred in a steeper shelf area where a surge has a smaller potential. Thus, shelf topography may dominate the surge changes expected from wind profile alterations. Note that the opposite effect occurs for storms landing in an area where the shelf topography becomes shallower with distance from the storm center; here, we would want a smaller sized storm with the maximum winds closer to the center.

When the storm size changes, there are other and much more subtle effects that can also ameliorate the storm surge. For example, a storm moving alongshore generates surges whose heights depend on distance of track from shore, relative to storm size. Now, if the track remains the same but relative distance changes due to changing storm size, then the surge heights will also change. We refrain from discussing many other such oceanographic effects.

REFERENCES

Gentry, R. Cecil (1970): Hurricane Debbie modification experiments, August, 1969. Science, 168, pp. 473-475.

Holliday, Charles (1969): On the maximum sustained winds occurring in Atlantic hurricanes. ESSA Technical Memorandum WBTM-SR-45, Fort Worth, Texas, 6 pp.

Jelesnianski, Chester P. (1966): Numerical computations of storm surges without bottom stress. Monthly Weather Review, 94, No. 6, pp. 379-394.

Jelesnianski, Chester P. (1967): Numerical computations of storm surges with bottom stress. Monthly Weather Review, 95, No. 11, pp. 740-756.

Jelesnianski, Chester P. (1972): SPLASH (Special program to list amplitudes of surges from hurricanes), Part 1, Landfall storms. NOAA Technical Memorandum NWS-TDL-46, Silver Spring, Maryland, 52 pp.

Lefschetz, S. (1962): Geometric Theory of Differential Equations. (Wiley, New York).

Myers, Vance A. and William Malkin (1961): Some properties of hurricane wind fields as deduced from trajectories. National Hurricane Research Report No. 49, U. S. Weather Bureau, Washington, D. C.,45 pp

Rosenthal, Stanley L. (1971): A circularly symmetric primitive-equation model of tropical cyclones and its response to artificial enhancement of the convective heating functions. Monthly Weather Review, 99, pp. 414-426.

Simpson, Robert H., M. R. Ahrens and R. D. Decker (1963): A cloud seeding experiment in Hurricane Esther, 1961. National Hurricane Research Project Report No. 60, U. S. Weather Bureau, Washington D. C., 30 pp.

APPENDIX A - MAXIMUM SURFACE WIND

The maximum surface wind of storms is not used directly as a parameter in our model because it is implicitly defined by ΔP and R. It is a distressingly difficult parameter to measure or observe, even its definition is open to question.

For a stationary storm, repeat stationary, we relate, for our storm model (Jelesnianski, 1966), the maximum wind W_M with ΔP and R, figure A1. Our maximum wind is an idealized[9] wind on a circle of radius R from the storm center. This relation is used in the dynamic surge model where we limit R to $10<R<50$ miles; i.e., we do not want to consider point vortex storms nor overly large storms compared with the average Continental Shelf width. For constant R, W_M varies as $(\Delta P)^{1/2}$, and for constant ΔP

[9]We assume that a continuous, well-behaved, wind profile results from a balance of forces, appendix C, and on this wind profile there exists one--and only one--maximum wind.

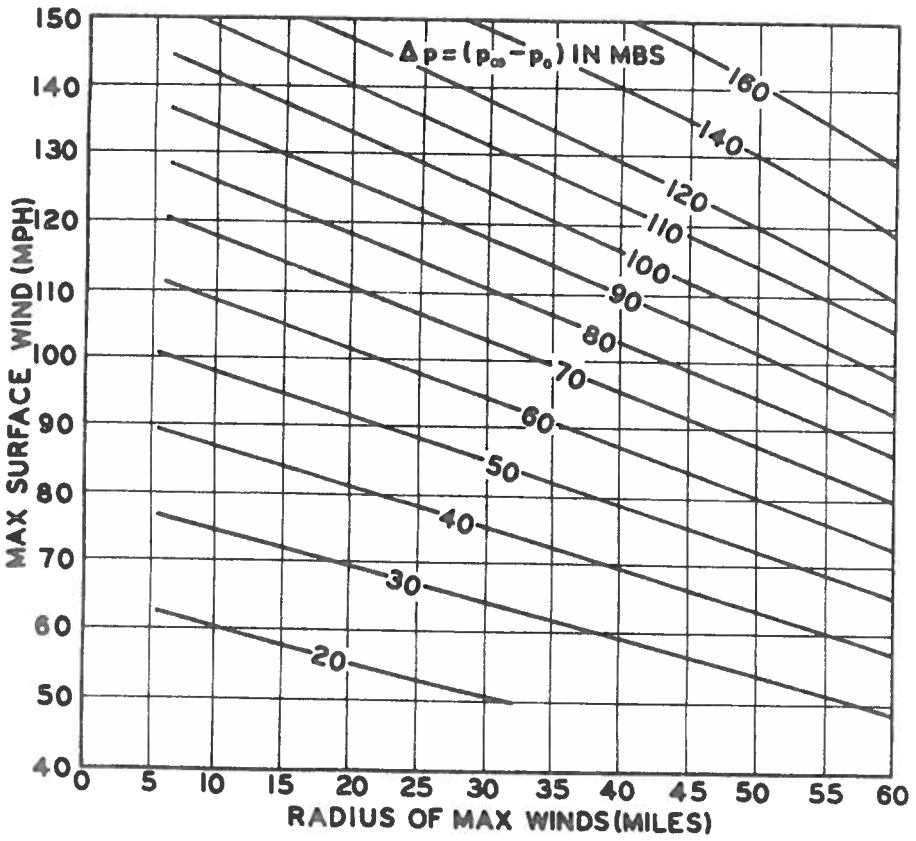

Figure A1. A nomogram relating three storm parameters for a stationary storm; the maximum wind W_M, the radius of maximum wind R, and the pressure drop of the storm ΔP. The storm center is at latitude 30°.

it varies linearly as mR+b, where m and b are functions of ΔP; these are rough estimates.

W_M is significantly smaller than the "fastest mile" wind currently employed by weather forecasters. This is shown in figure A2 where we compare W_M against an empirically derived curve of "fastest mile" wind (Holliday, 1969). Our W_M, plotted for latitude 30° only, varies with R as well as pressure.

These two winds represent different attitudes with respect to weather and surge forecasting. In weather, we are interested in a selected, local maximum wind for a measure of potential damage on small structures; thus, it is an end product. In surge forecasting, we view the wind as a means to an end, i.e., the generated surge. Except for very small effects, the local surge is not directly dependent on the local wind. For surge generation, we view our winds 'W' as long-time averages, that is winds without noise (i.e., gusts); for any ray from the

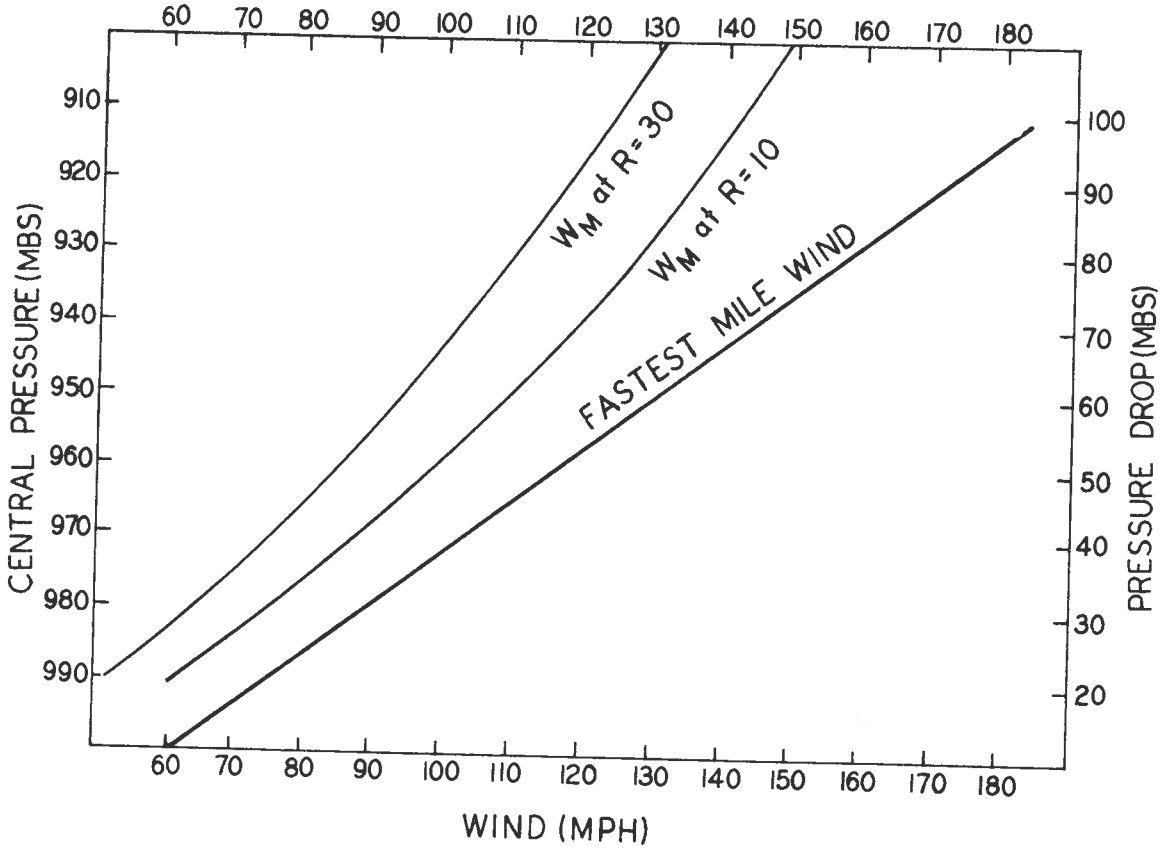

Figure A2. A comparison of the model storm maximum wind 'W' from figure A1 against an empirically derived 'fastest mile wind' (Holliday, 1969).

storm center the wind profile is the same[10]. Our model winds are neither spot measurements or measurements from small sampling periods, nor are they represented by Doppler winds measured on selected rays from the storm center. The observed winds for Hurricane Debbie--discussed in the main report, (fig. 3)--appear to have a noisy structure (gusts?); we do not permit such detail in our model wind profile and assume that the noisy structure of the winds end up as viscosity terms in equations of motion.

A "mile" wind measures the average speed for a mile of air passing wind measuring devices. The averaging time for this "mile" wind is an inverse function of the wind; as such it guarantees that gusty winds, imbedded in mile length parcels of air and properly oriented, will shorten the averaging time. Hence, the "fastest mile" wind is biased towards gusty wind speeds.

A wind speed measuring device fixed on the ground and sampling a moving storm can sample most any wind speed depending on the sampling time. For an extremely long sampling time, the average wind speed would be some number for, say, the general circulation; for an extremely short sampling time, the "fastest" average would be some number for extreme gusts. The "fastest mile" wind is an admirable compromise when dealing with the small structures, or even short gravity waves such as sea surf; however, it can be an erroneous picture when dealing with long gravity waves such as storm surges. Our W_M can be significantly smaller than winds averaged along selected segments of the storm, and faster on others.

The "fastest mile" winds of figure A2 are for moving, not stationary, storms. We remark that 1.3 W_M, for R=20 miles, closely parallels the empirically derived curve[11] up to a pressure drop of about 65 mb; this is a rough measure of the difference for the two winds. Note that we have not proved any direct connection between these winds. It would take a far more complete analysis to do that.

[10] In the model, we incorporate simple corrections for storm motions so that the upper maximum wind becomes $W_M + \frac{1}{2}$ the storm speed. Storm motion corrections are designed to become negligible at large distances from the storm center. It turns out that the generated surge is not sensitive to this correction except when storm speed approaches our W_M.

[11] Holliday (fig. A2) does not use the radius of maximum winds as a parameter.

APPENDIX B - CRITICAL STORM SIZES AND VECTOR STORM MOTIONS

A detailed mathematical analysis of the critical R in figure 2 would require more effort than seems justified for this report. What follows is a brief examination of some factors involved. We wish to emphasize that in deriving figure 2, a standard basin and a standard vector storm motion were used; hence, it does not apply to other basins or directions of storm motion.

We consider here three hypotheses that might plausibly explain the critical R of about 30 miles in figure 2.

1. The total available force on the sea--from wind stress--is a maximum when R is about 30 miles.

2. A critical situation occurs when storm diameter and shelf width are the same.

3. The transient state of surge dynamics in a fixed basin is such that vector storm motion plays a significant role.

We can compute, with our simple storm model, the total available force on the sea caused by wind stress; this is done with the wind profile of figure 1, plus the linear relation of W_M to R in figure A1. The maximum integrated force occurs with R lying between 70 to 90 miles, depending on pressure drop. This is only an approximation since inflow angle is ignored, the storm is stationary in an infinite sea, only magnitude and not direction of the force is considered, and the near linear relation from figure A1 is open to question with large storms. The first possibility is not a good choice to determine critical R. Empirical tests, with basins and storm motion other than standard, give different critical R's.

At first glance, it appears that the second possibility is a good choice because critical storm diameter and shelf width used in the model are nearly the same, but this turns out to be only coincidence. Empirical tests show that the peak surge computed by our model does not strongly depend on shelf width, providing the shelf width is at least greater than R and that the shelf-edge depth approaches or exceeds an Ekman depth. This is fortuitous, otherwise shelf width would be yet another parameter to contend with in forecasting surges, and one whose effects would not be well established.

A special case can exist with a very shallow basin of near constant depth and abutting a near vertical Continental Slope. For this case, energy transmissions across the shelf edge is discontinuous. Hence, a relation between storm diameter and shelf width could conceivably be a factor for critical R. We note that large storms at all times have a large part of their strong winds outside the shelf, but small storms--for some finite time duration--concentrate most of their strength on a

Figure B1. Contours of peak coastal surge values in feet. Circles are storm speeds, rays are crossing angles or storm track relative to the coast; for orientation the coast can be conceptually placed on the 0° — 180° vertical axis with sea to the right and land to the left. A standard basin and model storm are used. The separate diagrams from left to right are for storms with an 'R' of 15, 22.5, and 30 miles, respectively, and ΔP of 55, 62, and 68 mb, respectively; this makes the maximum wind 'WM' 100 mph in each diagram. For storms traveling nearly parallel to the coast, the contours are speculative because of transient wave effects. The small insert shows a coastal surge profile, at time of peak surge, with the observer on sea facing land; note the negative surges on the left side of the profile.

small area of the shelf. Now, if the energy for surge formation is produced while the storm is on the shelf, we expect an optimum R when total force exerted on the sea surface of the shelf is a maximum; i.e., when storm diameter and shelf width are identical.

Natural basins, however, are rarely shallow at the shelf edge; they are in fact deep. By deep, we mean compared with an Ekman's depth of about 300 ft, where downward diffusion of momentum from wind stress is small. This means that energy is transmitted across the shelf without reflections at its edge.

Empirical tests with the model show that the third possibility can account for the critical R. For a given basin, and a given storm size--no matter the fixed parameter ΔP--there is a critical vector storm motion that generates the highest peak surge on the coast. This is illustrated in figure B1 for three different storm sizes moving across a standard basin. For each ray or direction of storm motion, there is a critical storm speed that gives the highest peak surge (for storms traveling from land to sea and near normal to the coast, the critical speed is zero). Now note that the critical speed of most rays increases[12] with an increase in storm size; we assume this increase is continuous. The critical speed is a function of R; similarly, critical R turns out to be a function of storm speed, as seen in figure 2 which shows a critical R for constant storm speed.

A stationary storm eventually sets up an equilibrium sea surface whose coastal surges are highest when the storm center is on, or close to, the shore. An infinitely fast moving storm exerts no stress on the sea and hence no storm surges; because it takes time to diffuse momentum downward into the sea when generated by surface stress. We cannot assume that the stationary storm sets up the highest possible surge, for we would then ignore the dynamics of surge generated by a moving storm. The momentum field in the sea consists of two parts: a divergence part and a vorticity part. The divergence produces surges directly and travels more or less with the storm; the vorticity part in our linear model, however, cannot produce surges or travel until it is converted to divergence. This can de done slowly by the Coriolis effect or more quickly by the sloping depths of the Continental Shelf. Consequently, the faster the storm travels, the greater the spread of the two effects. If the storm is not moving too fast, then the potential surge generation is greatest when land-falling storms move toward shallow water (from sea to land) and least when moving to deeper depths (from land to sea); this is why we have a zero critical speed for storms moving from land to sea.

We remark that the basin is a factor for critical vector storm motion. If the slope of the depth profile is increased (decreased) then critical speed increases (decreases).

APPENDIX C - COMPUTING PRESSURE AND INFLOW ANGLE PROFILES FROM A GIVEN WIND PROFILE

Our storm surge model requires the fields of forces on the sea surface generated by tropical storms. The required information includes the wind speed and direction, and the surface pressure as a function of position. Since this massive quantity of data is generally unobtainable, we have adopted the policy of constructing a model wind profile and computing the pressure and wind direction for a stationary, symmetric storm; we then apply a correction term to the wind speed to approximate the asymmetry due to storm motion. Details are given in Jelesnianski (1966).

The pressure, wind speed, and wind direction for the stationary symmetric storm are not quite arbitrarily chosen. The pressure and direction are determined from the wind speed by a balancing of forces. The equations for this are presented in (Jelesnianski, 1966) and are reproduced here. They are adapted from Myers and Malkin (1961):

$$\frac{1}{\rho_a}\frac{dp}{dr} = \frac{k_s V^2}{\sin\phi} - V\frac{dV}{dr} \tag{1}$$

$$\frac{1}{\rho_a}\frac{dp}{dr}\cos\phi = fV + \frac{V^2}{r}\cos\phi - V^2\frac{d\phi}{dr}\sin\phi + k_n V^2. \tag{2}$$

Here ρ_a is the surface atmospheric density considered constant, $p(r)$ is the pressure, $\phi(r)$ the inflow angle, or angle toward the storm center, $V(r)$ is the wind speed; all are functions of r, the distance from the storm center. The terms k_s and k_n are empirically determined coefficients, representing stress coefficients in the directions opposite and to the right of the wind, respectively. These stresses are given by the coefficients times the square of the wind speed, and f denotes the Coriolis parameter.

Equations (1) and (2) are to be solved for $p(r)$ and $\phi(r)$, but the form of the wind speed[13] profile $V(r)$ must be known first. For the storm surge forecasting program SPLASH (1972), currently in use, the profile

$$V(r) = V_r\frac{2Rr}{R^2+r^2} \tag{3}$$

[13] In this appendix, V corresponds to W, and V_r corresponds to W_M as given in the main text.

has been adopted. The term, R, the "radius of max winds," is the distance from the center at which V(r) is greatest, and $V_r = V(R)$ is the value of that maximum wind speed.

Of course, many other profiles may be chosen. Equation (3) has the property of increasing wind speed from r=0 to a maximum at r=R, then decreasing back to zero. The same would hold if the term $\frac{2Rr}{R^2+r^2}$ were replaced by a function of itself, say

$$(\frac{2Rr}{R^2+r^2})^q \text{ or } \log\ (\frac{2Rr}{R^2+r^2} + 1) \text{ or } \exp 1 - \{\frac{R^2+r^2}{2Rr}\}.$$

In this report, we replace V(r) by an interpolated function between tabulated values of wind speed, obtained from Project STORMFURY experiments. For reasons of stability, which we discuss later, it is important to use an interpolation scheme that is continuously differentiable, which rules out the common Newtonian or Lagrangian schemes; all favor some such scheme as the spline curve.

The procedure for solving (1) and (2) for p(r) and $\phi(r)$, with a given wind profile has been a Runge-Kutta type integration scheme applied to a transformation of (1) and (2). The transformation reduced problems of instability associated with a straightforward application of the Runge-Kutta method. This procedure was stable for the wind profiles given by (3) and for commonly encountered values of V_r, R, and latitude, but not for extreme values. That is, it was only marginally stable.

Because STORMFURY experimental data deviates from the profile given by (3), it became clear that another, more stable computation technique would be required. An investigation was then opened to determine the reason stability was so difficult a task, and to design a new and more stable method.

Ironically, we found that a leading contributor to the instability of the Runge-Kutta integrating scheme was the extreme stability of the differential equations used. The extreme nature of the stability arises from the equations being singular at the storm center.

We proceed by eliminating the pressure from (1) and (2) and write $u = \cos\phi$ to obtain

$$\frac{du}{dr} = k_s \frac{u}{\sqrt{1-u^2}} - u\ (\frac{1}{V}\frac{dV}{dr} + \frac{1}{r}) - \frac{f}{V} - k_n \qquad (4)$$

The right side of (4) will be called the "slope function" $F(u,r)$. We shall consider a strip in the u,r plane $0 \leq r \leq \infty$, $0 \leq u \leq 1$. If F is continuous in the interior of the strip, then by the geometric theory of differential equations (Lefschetz, 1962), through every point u_0, r_0, in the interior of the strip passes one of the solutions $u(r)$ of (4). At $r = r_0$, that solution has the slope $\frac{du}{dr} = F(u_0, r_0)$. Thus, a graphic method of solving (4) is to place short lines of slope $F(u_0, r_0)$ through each point, then, guided by these slopes, trace the curves. Indeed, numerical methods of solving such equations can be regarded as highly precise applications of this procedure.

In all of our subsequent discussion, we assume the wind profile $V(r)$ to be a continuously differentiable function, that vanishes at $r=0$ and is bounded. Examining (4), we find that, for $u=0$, $F(u,r)<0$, while for fixed $r>0$, $F(u,r) \to +\infty$ as $u \to 1$. With fixed u, $0 \leq u < 1$, $F(u,r) \to -\infty$ as $r \to 0$.

The point $u=1$, $r=0$, which is the intersection of two lines on which $F = +\infty$ and $F = -\infty$, respectively, is of great interest. Because of the continuity of F in the interior, it follows that in any neighborhood of this point, however small, the slope function F takes on all values between $+\infty$ and $-\infty$. Such a point is an essential singularity; at this point, various principles of differential equations no longer apply.

Again because of the continuity of F, there is a smooth curve $u = u_0(r)$ on which $F(u,r)=0$. It extends from $r=0$ to $r=\infty$, and, for $r \neq 0$, $0 < u_0(r) < 1$. As $r \to 0$, clearly $u_0(r) \to 1$. We call this curve[14] the zero-slope curve. When traced to the right, all solutions of (4) slope upward when they are above the zero-slope curve; they slope downward when they are below it, and they are parallel to the r-axis when they cross the zero-slope curve.

In figure C1, we show the strip $0 \leq u \leq 1$, $0 \leq r \leq \infty$ for the wind profile of (3) with R = 30 miles, V_r = 100 miles/hr, and latitude is 30°N. The vertical scale has been stretched to emphasize the details for $u \approx 1$. Some of the solution curves for (4) have been traced in this figure.

In examining figure C1, remember that the entire strip is covered with solution curves, and only some of them are traced here. The theory of differential equations provides that solution curves satisfy these rules:

(1) Through every point where F is continuously differentiable passes one, and only one, solution curve.

[14] In some instances, other curves exist where $F(u,r)=0$. These are closed curves, containing a finite portion of the u,r plane not touching any portion of the boundary of our slope. They may safely be ignored in what follows.

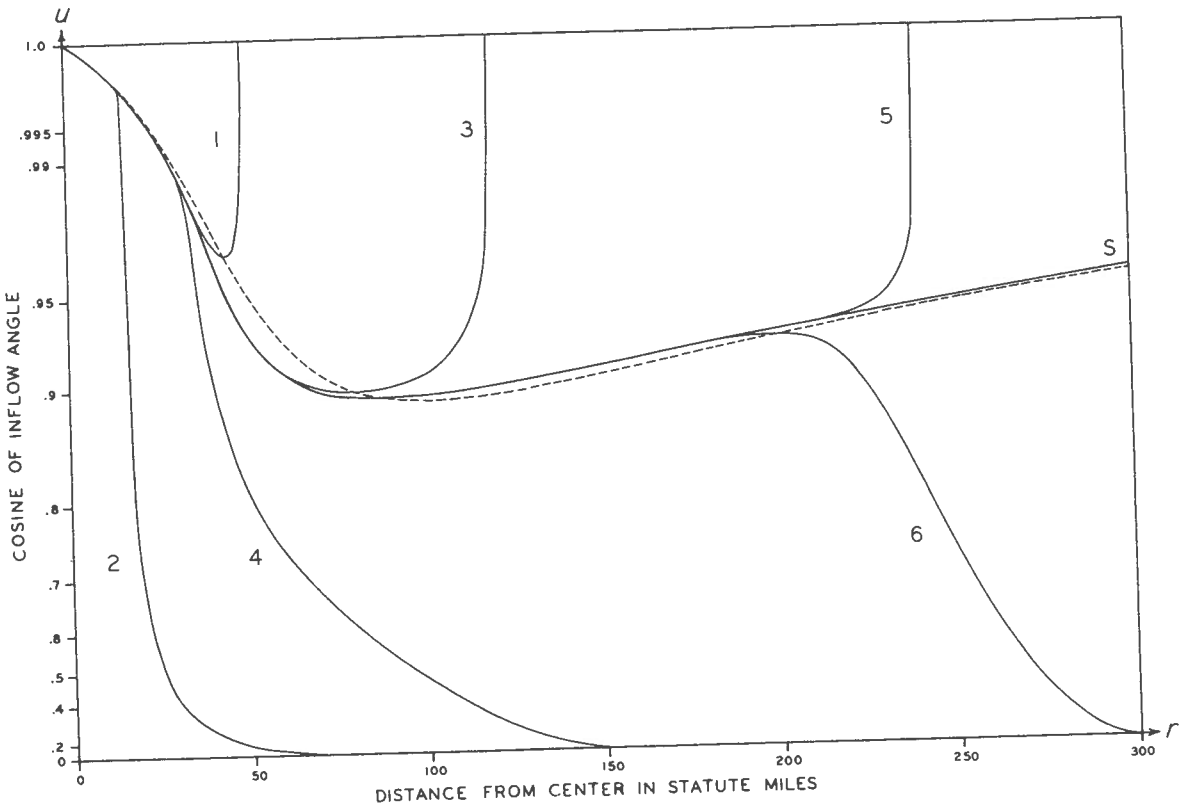

Figure C1. Some solutions to (4) inside the strip $0 \leq r \leq \infty$, $0 \leq u \leq 1$, where u is the cosine of inflow angle. The curve labeled 'S' is the only curve lying entirely inside the strip, and hence satisfies the 'boundary condition at ∞'. It corresponds to an analytic wind profile with parameters at V = 100 mph, R = 30 miles, latitude = 30°N. The vertical scale has been stretched to clarify details at the top of the strip.

(2) This solution curve may be extended to the left and to the right indefinitely, or until it encounters one of the boundaries of the strip, i.e., no solution curve ends in the middle of the strip.

(3) No two solution curves cross, or even meet, at any point where F is continuous; any solution curve that starts between two others remains between those two others. Furthermore, any two distinct curves are separated at all times by some length, however small.

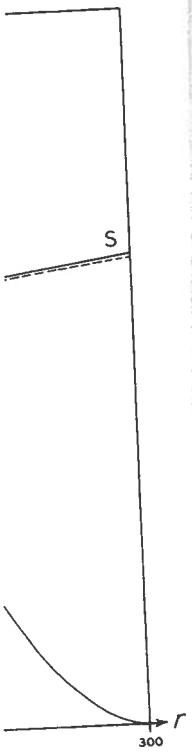

The dashed curve in figure C1 is the zero-slope curve; as mentioned earlier, above this curve all solution curves ascend when traced to the right; below it, they descend to the right.

On further examination of figure C1, it becomes clear that, if any two solution curves are traced to the left they quickly converge, becoming so close as to be nearly indistinguishable. This illustrates the high stability of the differential equation. Suppose, for example, a method of tracing solution curves is used to follow the particular curve marked S, and at r=200 miles, a momentary breakdown causes it to skip to a point midway between S and the curve marked 6. If it then follows the solution curves properly, the curve it traces will be squeezed between S and 6, becoming indistinguishable from S at about r=180 miles. Contrariwise, if the solution curves are traced to the right, a slight misstep causes a rapid deviation from the desired curve.

Again examining figure C1, we may suspect that, since the solution curves converge on each other so fast, they are all going to the same point. Indeed, it can be proved that all solutions to (4) pass through $u = 1$, $r = 0$, in apparent contradiction to rule (3) above. This contradiction, however, is only apparent, since F is not continuous at this point. Furthermore, it also turns out that all derivatives of any one solution at r=0 are equal to the corresponding derivative of any other solution. This makes it quite fruitless to attempt to specify a boundary condition at r=0, in terms of specifying a value for u or for its derivative at r=0.

In tracing a solution curve to the left, we see that the curve cannot pass through the top or the bottom of the strip. For, to arrive at the top, the curve must ascend above the zero-slope curve while running to the left, but above the zero-slope curve solution curves ascend only to the right. Similarly, to get to the bottom of the strip, the solution curves would have to descend below the zero-slope curve.

There is no such prohibition against solution curves through the top or bottom of the strip when traced to the right. Indeed, from figure C1, it appears that most of the curves do just this. Solution curves that pass through the top of the strip take on values of $u = \cos\phi > 1$, and do not correspond to real inflow angles.

Solutions that pass through the bottom take on values of $u = \cos\phi < 0$, corresponding to anticyclonic flow for all values of r larger than the crossover point. This might be conceivable, but further analysis shows that such a curve would soon pass through $u = \cos\phi = -1$ and again real inflow angles would not exist.

Thus, for a solution to be physically valid, it must remain within the strip for all r, i.e., $0 < u(r) < 1$ for $r > 0$. It turns out that there is one and only one solution curve with this property, which must be taken as our "boundary condition" imposed at "$r = \infty$". This curve has been labeled "S" in figure C1.

For practical reasons, we do not actually start at $r = \infty$, but select an arbitrary initial condition at some point r_0, much larger than the values of r in which we are interested. We then trace this solution curve to the left, being assured in the first place that the solution curve will remain in the strip $0 < u < 1$, and in the second place, that it will rapidly converge on S, being practically identical with S well before values are required.

Having seen that the singularity at $u = 1$, $r = 0$ makes (4) a most unusual boundary value problem, let us take up again the question of integration schemes. The derivation of the various Runge-Kutta schemes of integration rests on smoothness assumptions of two types: (a) the assumption that the solution curves u(r) have derivatives to certain orders, and these derivatives do not change greatly in the length of an integration step Δr, and (b) the assumption that the slope function F(u,r) has derivatives to certain orders, and these derivatives do not change greatly in the course of changes in r of amount Δr, and in changes in u of amount $|F|\,\Delta r$ (i.e., in the amount u would change while tracing solution curve one integration step).

When we examine curve "S" of figure C1, assumption (a) seems quite plausible. However, assumption (b) refers, not only to points on a solution curve, but also to points on either side of a solution curve, and we must examine it carefully. Consider, in particular, the derivative $\frac{\partial F}{\partial u}$. This expresses the rate with which the slope function is increasing as you go from one solution curve to a nearby one, with fixed r. If you consider two nearby solution curves in a region where $\frac{\partial F}{\partial u} > 0$, the higher curve is descending to the left more rapidly than the lower (or the lower is ascending more rapidly than the higher) so that the curves converge, as in figure C1. Hence, $\frac{\partial F}{\partial u}$ is an indication of stability of the differential equations and if $\frac{\partial F}{\partial u} >> 0$ the curves converge extremely fast; therefore, we call the differential equation highly stable.

The term $\frac{\partial F}{\partial u}$ can measure the curvature of the solution curves. For, by the chain rule, we have $\frac{d^2u}{dr^2} = \frac{d}{dr} F(u,r) = \frac{\partial F}{\partial u}\frac{du}{dr} + \frac{\partial F}{\partial r} = F\frac{\partial F}{\partial u} + \frac{\partial F}{\partial r}$ for any soltuion of $\frac{du}{dr} = F(u,r)$. Assumption (b) above states that the derivatives of F, and hence the curvatures of the solution curves, do not change rapidly as we go from one solution curve to a nearby one. Now compare curves "S" and "2" of figure C1. At the point where curve "2" stops rising sharply and turns to parallel "S" (r = 16 miles), the curvature is extremely sharp and concave. However, curve "S" is only mildly curved, and concave. This demonstrates dramatically that the curvatures do change rapidly as we move from one solution curve to another nearby one. Consequently, we must reject assumption (b).

We decided to modify a Runge-Kutta type scheme by removing its dependence on assumption (b) above. For the particular case of equation (4), this turned out to be fairly easy.

First, a change of variable was made for (4). We write $w = Vru = Vr \cos \phi$, and (4) becomes

$$\frac{dw}{dr} = \frac{k_s w V r}{\sqrt{V^2 r^2 - w^2}} - fr - k_n Vr. \qquad (5)$$

We write the right side of (5) as G(w,r), the slope function for w. In the new coordinate system, the solution curves from figure C1 appear as in figure C2. The dashed curve in figure C2 does not correspond to that in figure C1. It is the zero-slope curve for w, G(w,r) = 0. The other curves, however, do correspond. The uppermost curve is w = Vr or u = cos ϕ = 1; values of w above it correspond to u = cos ϕ > 1 and do not correspond to real angles.

Figure C2 is not as useful for exposition as figure C1. For instance, it is not as clear that, for r→0, u = cos ϕ→1 and the inflow angle becomes zero at the center of the storm. Nevertheless, it is clear that our considerations above still apply on figure C2 as strongly as on figure C1.

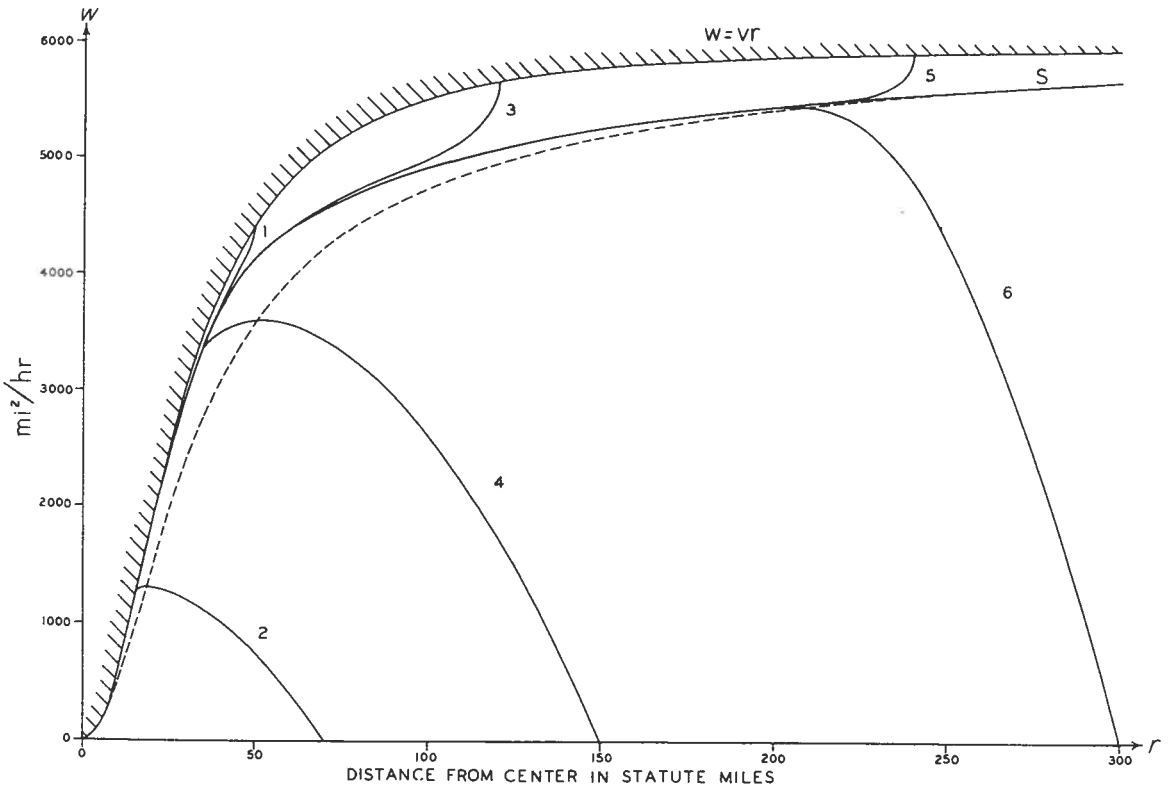

Figure C2. Some of the solutions to (5) in the r-w plane, where w = V r u = V r cos ϕ. The solution curves correspond exactly to those of (4), figure C1; however, the zero-slope curve does not correspond to that of (4).

Equation (5) has several computational advantages. In the first place, it does not explicitly involve derivatives of $V(r)$, which is a considerable advantage when working with a curve interpolated through tabulated values. In the second place, $\frac{\partial G}{\partial w} > 0$ without exception, whereas there are some conditions where $\frac{\partial F}{\partial u} \leq 0$ in local regions. The important usefulness of this property will develop shortly.

Let us suppose we are tracing a solution curve from right to left, and at the point $r_k = k\Delta r$ we have attained a value for w of w_k. We wish to trace the curve one more step, to $r = r_{k-1} = (k-1)\Delta r$ where $w = w_{k-1}$. At r_k, the curve has the slope $G(w_k, r_k)$, and at r_{k-1} the curve should have the slope $G(w_{k-1}, r_{k-1})$. If we assume that $\frac{d^2w}{dr^2}$ is slowly varying over this range of r, i.e., that w(r) may be adequately represented by a parabola, then we have the relationship

$$\frac{w_k - w_{k-1}}{\Delta r} = \tfrac{1}{2}(G(w_k, r_k) + G(w_{k-1}, r_{k-1})); \qquad (6)$$

i.e., the average slope over the interval (r_{k-1}, r_k) is the average of the two slopes. Equation (6) might be used to evaluate w_{k-1}, except for the fact that $G(w_{k-1}, r_{k-1})$ is not known until w_{k-1} is known.

The Heun method, one of the simplest Runge-Kutta methods, uses (6) to evaluate w_{k-1}, but approximates $G(w_{k-1}, r_{k-1})$ with $G(\tilde{w}_{k-1}, r_{k-1})$ where

$$\frac{w_k - \tilde{w}_{k-1}}{\Delta r} = G(w_k, r_k),$$

i.e., by extrapolation on the line passing through w_k, r_k with slope $G(w_k, r_k)$. The justification for this relies on assumption (b) above, and is not valid for our purposes.

Our modification consists in treating (6) as an algebraic equation to solve for w_{k-1}, when the w_k, r_k, and r_{k-1} values are known.

Now, the left side of (6) is a linear function of w_{k-1}, with slope $-\frac{1}{\Delta r}$, while the right side is a monotone, increasing function of w_{k-1}, with positive derivatives $\frac{\partial G}{\partial w}$ and curvature $\frac{\partial^2 G}{\partial w^2}$ for $w_{k-1} > 0$. Figure C3 shows a typical situation. The roots of (6) occur when the two curves of figure C3 cross, which clearly can occur at only one point. The importance of this fact is that no decision procedure need be devised

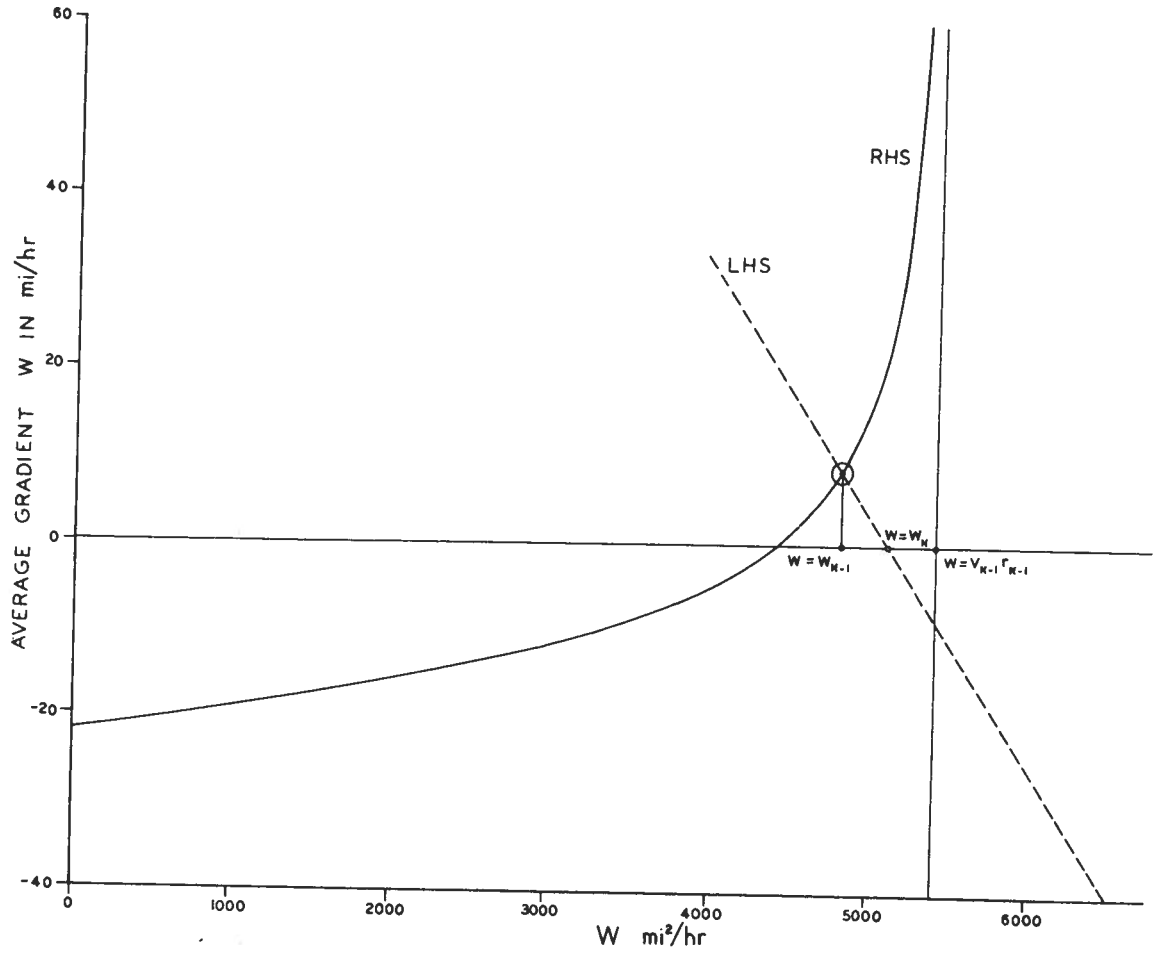

Figure C3. Illustration of the solution to (6) for the fundamental step in our finite difference method; this corresponds to a step size of 35 miles, between r_k = 125 miles and r_k = 90 miles. The large step size is chosen to clarify details. The new value of w, w_k, is located where the curve and line cross. The curve has an asymptote at $w = V_k r_k = V(r_k) r_k$.

to determine which root to use. The importance of the fact that $\frac{\partial^2 G}{\partial w^2} > 0$ for $w > 0$ is that the very fast Newton-Raphson method can be used to find the root, provided only that care is used to ensure that each iteration lies between $w = 0$ and $w = V(r_{k-1}) r_{k-1}$. If the root w_{k-1} of (6) is actually less than zero, this would imply that the finite difference scheme is not properly following the solution curve, and a smaller Δr would increase the slope of the straight line in figure C3 and change the position of the asymptote, but not the y-intercept of the curve; clearly it would ensure $w_{k-1} > 0$. In practice, however, there has been no need to change the step size Δr on this account.

Having solved (6) for w_{k-1}, we can now use this value and equation (6) (replacing k with k-1) to find w_{k-2} at $r_{k-2} = (k-2)\Delta r$, and so forth, in the usual manner. The resulting scheme is stable because the curves in figures C1 and C2 were drawn using it.

The accuracy of the present scheme has not been completely determined. It is plausible that, since (6) is derived by ignoring third-order terms, the errors from it are of order $(\Delta r)^3$ for each integration step, and, since the number of integration steps varies inversely with Δr, the accumulated error should be of order $(\Delta r)^2$. This estimate may be too pessimistic, however, for the property of the differential equation of squeezing the solution curves together applies also to stable finite difference approximations of it; hence, after some point the errors should diminish as fast as, or faster than, they accumulate.

A pragmatic test for accuracy lies in trying out the integration schemes for values of, say, Δr = 1 mile, 0.1 mile, 0.02 miles, and determine the magnitude of any changes in the results. Presumably the more accurate results are for the smaller step sizes. Such a test was conducted for the exceptional case of V_r = 200 mph, R = 5 miles, latitude = 5°N and the profile of (3). In proceeding from Δr = 1 mile to Δr = 0.1 miles, the maximum change took place at r = 10 miles. It amounted to 0.7° shift in inflow angle out of 2.853°[15], a relative shift of 23 percent; for r > 15 miles, there was no change to four significant digits, and, for r < 5 miles, the two profiles agreed to two significant digits. In the region 5 miles < r < 15 miles, the inflow angle is undergoing the most abrupt changes in the entire range of interest, and it is consequently more difficult to trace the solution. In proceeding from Δr = 0.1 mile to Δr = 0.02 miles, the greatest change again occurred at r = 10 miles. It amounted to 0.011°, a relative shift of 0.4 percent. Elsewhere, the agreement was to at least three significant digits, and to four significant digits in almost all cases. Hence, it appears that a step length of 0.1 mile is generally quite adequate, and indeed 1 mile is often sufficient.

Having found u(r), and hence $\phi(r)$, it is easy to use (1) to find the pressure p(r). Indeed, a simple trapezoid rule integration procedure appears to be quite sufficient.

For tabulated data such as given by the STORMFURY project, one consideration turned out to be quite important. Conventional procedures for interpolating between data points, such as the Newton or Lagrangian interpolation schemes, do not ensure that the interpolating curve has a continuous derivative across tabulated points. Thus, they generally allow a jump in the slope $\frac{dV}{dr}$ of the wind profile across a tabulated point. Now, it will be discovered in differentiating (5) that the curvature $\frac{d^2w}{dr^2}$ also undergoes a jump of amount

[15]The maximum inflow angle for this example occurred at r = 23 miles and was ϕ = 28.64°. Relative to this value, the shift was 2.3 percent.

$$- \frac{k_s w^3 r}{(V^2 r^2 - w^3)} \; 3/2 \; - k_n r$$

times the jump in $\frac{dV}{dr}$. For $w \approx Vr$, which occurs near the center of the storm, this becomes extremely large. Now, recall that (6) was derived on the basis that the curvature $\frac{d^2u}{dr^2}$ did not change greatly in the interval $r_{k-1} < r < r_k$. In consequence, for a wind profile with discontinuous slope, (6) may give quite erroneous values. Indeed, when a Lagrangian interpolation scheme was used, explosive instability in fact developed, immediately after one or another of the tabulated data points.

To avoid this source of difficulty, a cubic spline curve interpolation scheme was used instead. Such an interpolation scheme uses an interpolation curve whose first and second derivatives are continuous everywhere. With this scheme, no instability appeared whatever with the STORMFURY project data.